A Regenerative Pseudonoise Range Tracking System for the New Horizons Spacecraft

Richard J. DeBolt, Dennis J. Duven, Christopher B. Haskins, Christopher C. DeBoy, Thomas W. LeFevere, *The John Hopkins University Applied Physics Laboratory*

BIOGRAPHY

Richard J. DeBolt is the lead engineer for the New Horizons Regenerative Ranging Circuit. He received a B.S. and M.S. from Drexel University in 2000 both in electrical engineering. He also has received a M.S. from John Hopkins University in 2005 in applied physics. He joined the Johns Hopkins University Applied Physics Laboratory (APL) Space Department in 1998, where he has tested and evaluated the GPS Navigation System for the TIMED spacecraft. He is currently testing and evaluating the STEREO spacecraft autonomy system.

Dennis Duven received a B.S., M.S., and Ph.D. degrees in Electrical Engineering from Iowa State University in 1962, 1964, and 1971, respectively. He was responsible for coordinating and teaching the introductory Automatic Control Systems sequence at Iowa State from 1965-1973. Dr. Duven has been employed by the Space Department of the Johns Hopkins University Applied Physics Laboratory (APL) since 1973. His responsibilities at APL have included analysis and design of the SATRACK I and II missile tracking systems, a Miss Distance Measurement System for the SDI Brilliant Pebbles Program, an autonomous GPS Navigation System for the NASA TIMED satellite, and the Regenerative Ranging System described in this paper.

Chris. Haskins is the lead engineer for the New Horizons uplink receiver. He received a B.S. and M.S. from Virginia Tech in 1997 and 2000, both in electrical engineering. He joined the Johns Hopkins University Applied Physics Laboratory (APL) Space Department in 2000, where he has designed RF/Microwave, analog, and mixed-signal circuitry and subsystems in support of the CONTOUR, STEREO, and MESSENGER spacecraft. He also served as the lead engineer for the development of RF ground support equipment for the CONTOUR spacecraft. Prior to working at APL, Mr. Haskins designed low cost commercial transceivers at Microwave Data Systems

Chris DeBoy is the RF Telecommunications lead engineer for the New Horizons mission. He received his BSEE from Virginia Tech in 1990, and the MSEE from the Johns Hopkins University in 1993. Prior to New Horizons, he led the development of a deep space, X-Band flight receiver for the CONTOUR mission and of an S-Band flight receiver for the TIMED mission. He remains the lead RF system engineer for the TIMED and MSX missions. He has worked in the RF Engineering Group at the Applied Physics Laboratory since 1990, and is a member of the IEEE.

Thomas W. LeFevere is a digital design engineer in the Space Instrumentation Group at JHU Applied Physics Laboratory. He received his BSEE from Rutgers University in 1973 and MSCS from the Johns Hopkins University in 1987. He has designed numerous spacecraft instrument subsystems, Command and Data Handling subsystems and ground support testbeds over his 19 years at APL.

ABSTRACT

A pseudonoise regenerative ranging tracker has been developed as part of the telecommunications system for the NASA New Horizons Mission to Pluto and the Kuiper Belt. The New Horizons spacecraft pushes the boundaries of many space technologies to meet the unique demands of the mission over extreme distances. The long Earth-ranges at which the New Horizons spacecraft must operate will test the limits of conventional turn-around tone ranging, which has been the standard in most interplanetary missions. In addition to conventional tone ranging, the New Horizons telecommunications team has implemented a pseudonoise regenerative range tracking circuit as part of the spacecraft's digital receiver. The regenerative ranging circuit locks to a pseudonoise, high-rate, digital signal that has been modulated onto the

uplink carrier by the ground station. It then constructs a low-noise replica of the received pseudonoise code and modulates the downlink carrier with this reconstructed replica. The regenerative ranging system provides a substantial reduction of noise in the returned ranging signal and results in more accurate ranging results and/or shorter-range acquisition times. From an operations viewpoint, regenerative ranging reduces the complexity of setting up and conducting a ranging campaign, with fewer control parameters and shorter view periods. This paper will briefly discuss the theoretical and analytical development of the regenerative ranging circuit. The implementation of the regenerative ranging design within a single FPGA and its predicted mission performance will also be detailed.

INTRODUCTION

The New Horizons program is a NASA sponsored mission to characterize the geology and atmosphere of Pluto. The Johns Hopkins University Applied Physics Laboratory was chosen to design, test and build the New Horizons spacecraft. New Horizons is projected to launch in January of 2006 and is expected to fly-by Pluto in July of 2015. After launch the spacecraft will follow a heliocentric orbit to a rendezvous with Jupiter in 2007. The Jupiter encounter will provide a gravity assist to the spacecraft, which will send it on its 8-year cruise to Pluto. An extended mission would allow for fly-bys of any Kuiper Belt Objects (KBO) along the spacecraft's trajectory. Kuiper Belt Objects are numerous small planetoids found in the outer solar system. A graph of the planned mission trajectory for the New Horizons mission is shown in figure 1.

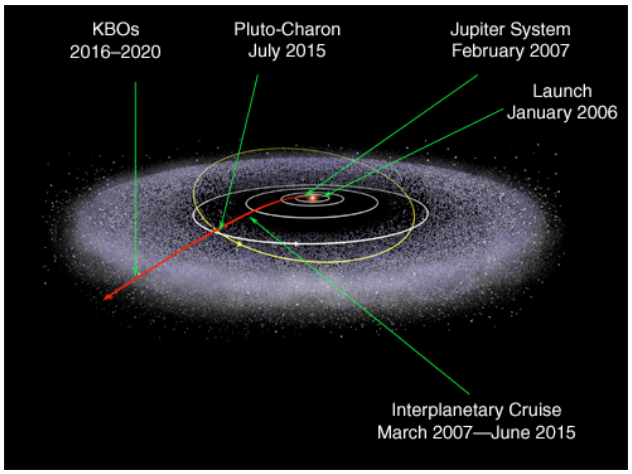

Figure 1. Mission Trajectory

The great distances to Pluto as well as any KBO encounters beyond Pluto pose many challenges for any communications or ranging system. The average distance to Pluto is 39 AU. (1 AU = ~ 150 million km); the round trip light time (RTLT) to a spacecraft at Pluto is over 8 hours. In the face of such long distances it is advantageous to have a ranging system that can remove almost all the noise accumulated by the uplink signal as it makes its way to the spacecraft. The regenerative ranging circuit on New Horizons will have this capability. In addition, due to the characteristics of the pseudonoise code used by the regenerative ranging system, the coordination of a ranging campaign is simplified and the impact on operations is reduced. [4]

This paper will discuss the implementation of a regenerative ranging pseudonoise tracker designed for the New Horizons spacecraft. This paper starts with a brief overview of the telecommunications system in which the regenerative ranging system resides. The theory of operation of the regenerative ranging circuit is then presented. A discussion of the implemented circuit and its test results concludes the paper.

OVERVIEW OF THE NEW HORIZONS TELECOMMUNICATIONS SYSTEM

A block diagram of the New Horizons RF Telecommunications System is shown in Figure 2.

Integrated Electronics Module (IEM)— Major electronic functions of the New Horizon spacecraft are housed in an integrated electronics module (IEM). These functions include the command and data handling system, the instrument interface circuitry, the telemetry interface function, the solid state recorder, and the receiver and exciter sections of the telecommunications system, along with the DC-DC converters that power them all. The integrated implementation reduces overall harness requirements and results in mass and cost savings. Two redundant IEMs are included on the spacecraft.

Each IEM includes Uplink, Downlink, and Radiometrics cards for telecommunications. The Uplink Card provides the command reception capability, as well as a fixed downconversion mode for an associated uplink radioscience experiment (REX). Since at least one Uplink Card must be powered at all times, the very low power consumption (2.3 W secondary) of this digital receiver has been an enabling technology for the mission. The Downlink Card is the exciter for the Traveling Wave Tube Amplifiers (TWTAs), and encodes block frame data from the spacecraft Command and Data Handling (C&DH) system into rate 1/6, CCSDS Turbo-coded blocks. It also calculates and inserts navigation counts into the frame data to support the noncoherent Doppler tracking capability, and is used to transmit beacon tones during cruise periods. The Radiometrics Card contains the REX and Regenerative Ranging Functions.

Ultrastable Oscillators (USOs) —Two 30.0 MHz USOs provide the ultimate frequency reference for the Uplink and Downlink Card local oscillators and clocks. The USOs are cross-strapped with a transfer switch and power splitter to retain redundancy in the Uplink and Downlink Cards in the event of a USO failure.

RANGING THEORY OF OPERATION

Traditional Metric Tracking. Metric tracking of interplanetary spacecraft has traditionally been accomplished with the system illustrated in Figs. 3(a,b) (see Refs. [1,2,3]). In this system, the Deep Space Network (DSN) transmits a high accuracy phase-modulated carrier to the spacecraft. A transponder on the spacecraft: (a) receives the DSN transmitter signal with time delay equal to the uplink range divided by the speed of light, (b) amplifies and demodulates the received signal, (c) translates the received carrier frequency up by a factor of 880/749, (d) passes the demodulated ranging signal through a low-pass filter (LPF) with a bandwidth of approximately 1 MHz, (e) phase modulates the new carrier with the output of the LPF, and (f) transmits this newly generated signal to a (possibly different) DSN receiver. This signal arrives at the DSN receiver with additional delay equal to the downlink range divided by the speed of light. The DSN receiver down-converts, amplifies, and demodulates the received signal, and then estimates two-way range from the delay between the transmitted and received modulation signal and two-way range-rate from the Doppler shift in the received carrier frequency. The ranging signal is typically a sequence of sine or square-wave tones with frequencies that periodically decrement from a starting value of approximately 1 MHz to a minimum value of a few 10s of Hz. The recovered range measurements will be ambiguous by the product of the speed of light times the period of the lowest frequency ranging tone used. If this ambiguity level is substantially larger than the uncertainty in prior knowledge of the two-way range, then the measurements can be treated as unambiguous. The measurements will also have measurement errors that are random with 1-σ noise levels proportional to the period of the highest frequency tone used and inversely proportional to the square-root of the product of the received signal-to-noise ratio (SNR) and the integration time used in the DSN receiver.

Unfortunately on long-range missions such as New Horizons, the uplink SNR is sufficiently low that the output of the spacecraft demodulator contains more noise than signal, and since the bandwidth of the LPF must be approximately 1 MHz (in order to pass the highest frequency ranging tone), most of that noise is passed-on to the downlink phase modulator. The result is a reduction by several 10's of dB in SNR at the DSN receiver necessitating a substantial increase in the receiver

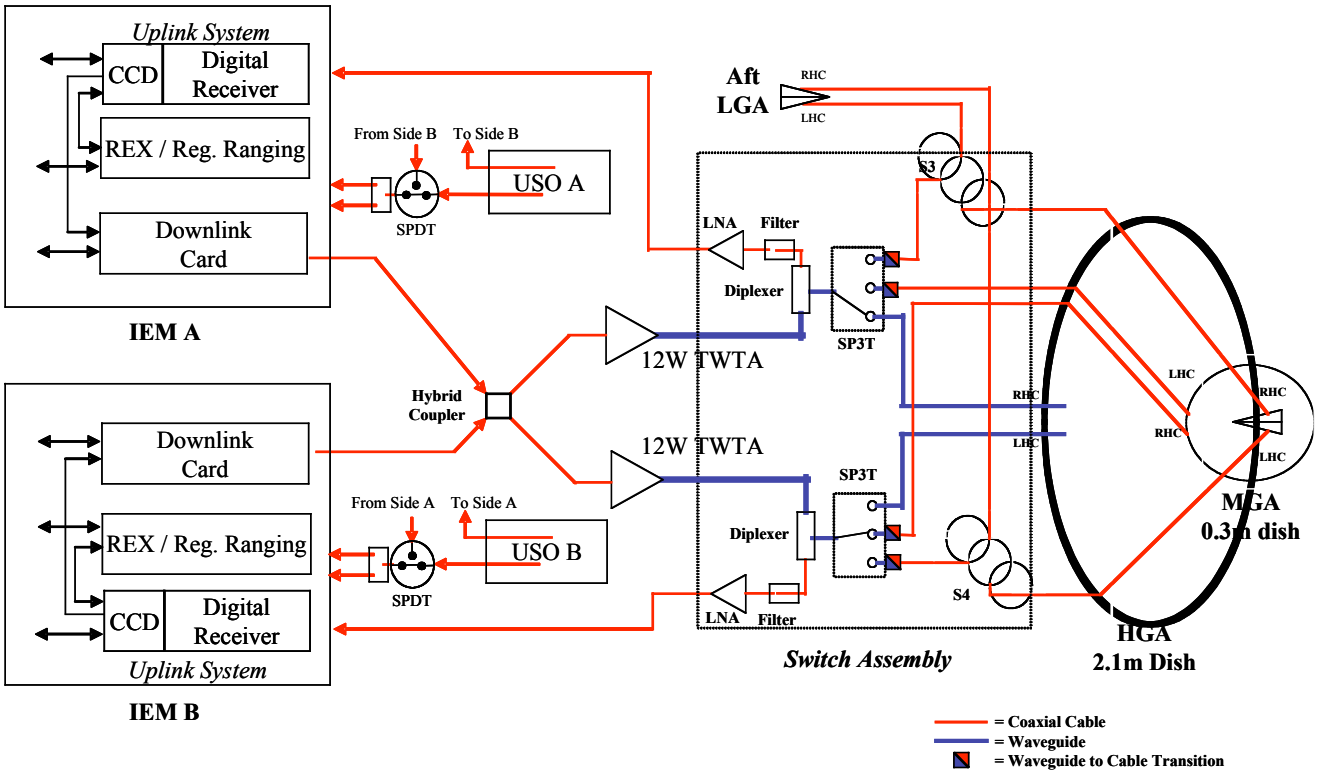

Figure 2. RF Telecommunications System Block Diagram

integration time to get two-way range measurements that satisfy mission accuracy requirements.

Regenerative Ranging. (See Refs. [4,5,6]). With its regenerative ranging option, New Horizons will have the means to eliminate most of the noise on the signal going to the downlink modulator. The regenerative ranging system uses an on-board delay-locked loop (DLL) to track the uplink ranging signal and regenerates a low-noise replica of that signal for the downlink modulator.

The DLL will have a tracking bandwidth of only 1 Hz (or 0.25 Hz if the narrowband tracking option is selected) as compared to a bandwidth of 1 MHz for a traditional transponder, so the uplink noise is almost totally eliminated.

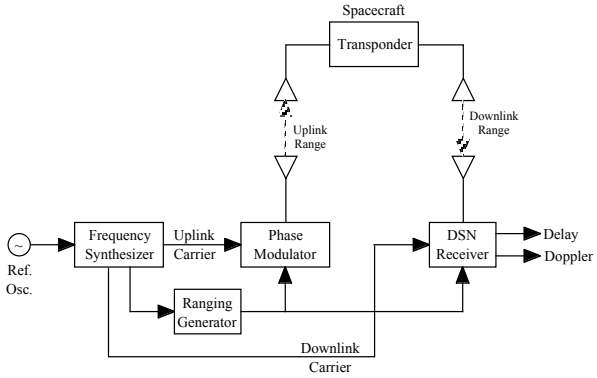

Figure 3(a). Block diagram of a traditional NASA metric tracking system.

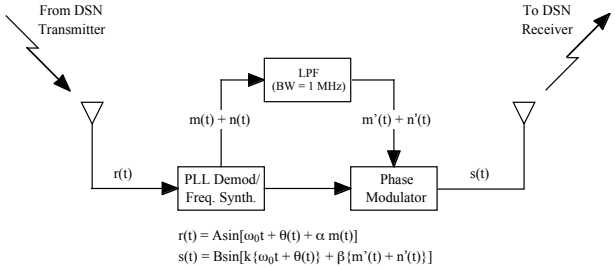

Figure 3(b). Signal processing block diagram for a traditional NASA transponder.

To facilitate the regenerative process, we follow reference [5] in introducing a pseudorandom noise (PRN) format for the ranging code. The code consists of a continuing string of approximately half-microsecond bipolar chips, C(i), whose signal value randomly alternates between two possible values of ±1. The chip sequence is generated from a corresponding sequence of logical bits, B(i), according to the equation C(i) = 2B(i) – 1. The bit sequence is defined by the equation

$$B(i) = B_1(i) \mid [B_2(i) \,\&\, B_3(i) \,\&\, B_4(i) \,\&\, B_5(i) \,\&\, B_6(i)], \quad (1)$$

where the terms $B_1(i) – B_6(i)$ represent the logical state of a set of six component generators defined by the equations

$$B_1(i) = [1,0] \quad (2a)$$

$$B_2(i) = [1,1,1,0,0,1,0] \quad (2b)$$

$$B_3(i) = [1,1,1,0,0,0,1,0,1,1,0] \quad (2c)$$

$$B_4(i) = [1,1,1,1,0,0,0,1,0,0,1,1,0,1,0] \quad (2d)$$

$$B_5(i) = [1,1,1,1,0,1,0,1,0,0,0,0,1,1,0,1,1,0,0] \quad (2e)$$

$$B_6(i)=[1,1,1,1,1,0,1,0,1,1,0,0,1,1,0,0,1,0,1,0,0,0,0]. \quad (2f)$$

[5]

The left-most bit in each defining sequence corresponds to an i value of 1, and i increases by one as we move to the right. When the right-most bit of a sequence has been reached the sequence recycles back to the left-most bit. The process results in a composite chip sequence with a period of 1,009,470 chips. The chips are generated at a rate proportional to the RF carrier frequency, the constant of proportionality being R = 221/(32*23968) chips/cycle. For New Horizons, the RF carrier frequency will be 7182.043388 MHz and the chip rate will be 2,069,467.087 chips/second.

The chip sequence generated by this scheme turns-out to be somewhat regular since the "and" of components 2-6 is zero most of the time. The composite sequence is therefore dominated by $B_1(i)$ which is an alternating sequence of 1's and 0's. This situation is acceptable for the New Horizons mission since code-division multiple access is not required. In addition, it actually helps decrease the tracking noise because a substantial amount of sideband power goes to the highest frequency (≈1 MHz) spectral lines. It also turns-out that the cross-correlation between C(i) and $C_k(i)$, the bipolar form of the k^{th} component generator, has an interesting and useful property as shown in Fig. 4. This property results in a substantial decrease in the acquisition time for the spacecraft's code generator since the search space is limited to the relatively short repetition interval of the component generators rather than the long repetition interval of the composite code.

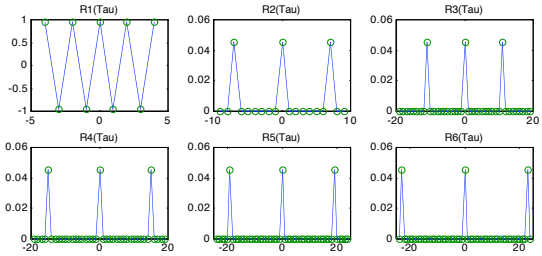

Figure 4. Cross-correlation plots for the composite code C(i) with the component generators $C_k(i)$.

A continuous-time signal, m(t), is generated from the chip sequence by replacing each chip with the product of C(i) times a half-sine pulse with a peak value of one and duration equal to the duration of the C(i) chips. The resulting string of half-sine pulses becomes the modulating signal for the RF carrier. A typical example of m(t) is shown in Fig. 5. The modulation index for New Horizons will be $\beta = 0.8$ radians.

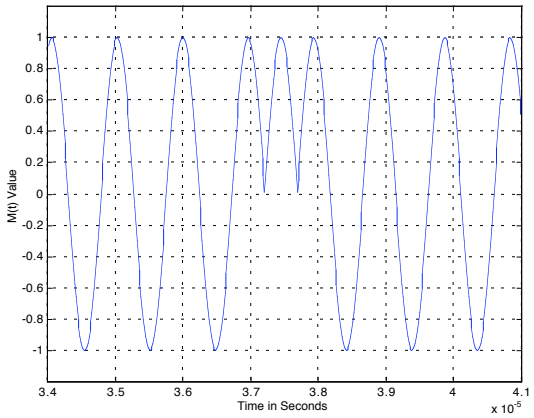

Figure 5. Typical example of a portion of the pseudorandom modulating signal, m(t).

Uplink Receiver. The uplink receiver for New Horizons performs three tasks – reception of uplink data and commands, two-way noncoherent range-rate measurement (see Refs. [7,8]), and conventional two-way ranging. The receiver also provides an output signal that serves as the input to the regenerative ranging circuit (RRC). The receiver has a two-stage super-heterodyne configuration with IF frequencies of 240 MHz and 2.5 MHz. The receiver uses feedback control of the local oscillators so that the 2nd IF output carrier will be phase locked to an internal reference derived from the spacecraft's 30 MHz ultra-stable oscillator (USO). A block diagram showing the portions of the receiver that pertain to the regenerative ranging function is shown in Fig. 6. Digital signal processing techniques are used extensively for improved accuracy and reduced power consumption.

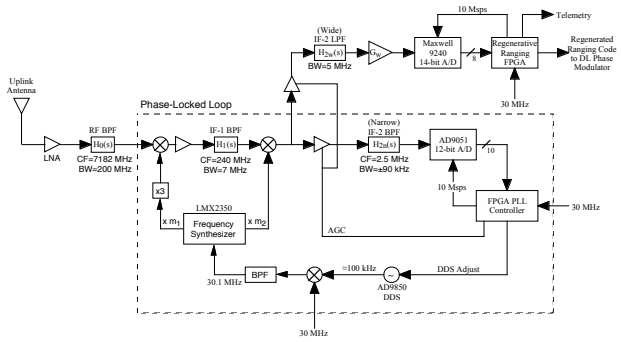

Figure 6. Block diagram of the uplink receiver and RRC.

Uplink Signal Processing. The received uplink signal will be

$$r(t) = A\sin\{\omega_0 t + \theta(t) + \beta\, m[t - \delta(t)]\}, \qquad (3)$$

where ω_0 is the uplink carrier frequency (in rad/sec), $\theta(t) = -(w_0/c)r_u(t)$ is the phase shift of the uplink carrier due to propagation delay, $\delta(t) = (1/c)r_u(t)$ is the uplink delay, and $r_u(t)$ is the uplink range. The uplink receiver phase-locked loop (PLL) will generate an effective local oscillator signal of the form

$$\ell(t) = 2\cos[(\omega_0 - \omega_2)t + \varphi(t)], \qquad (4)$$

where $\omega_2 = 2\pi$ x 2.5 MHz and $\varphi(t)$ is the receiver's estimate of $\theta(t)$ [and if the receiver is locked, then $\varphi(t) \approx \theta(t)$]. This produces a 2nd IF signal at the input to the RRC of the form

$$s(t) = A\sin\{\omega_2 t + \eta + \beta\, m[t - \delta(t)]\}, \qquad (5)$$

where η is the phase difference between the output of the wideband filter, $H_{2w}(s)$, and the output of the narrowband filter, $H_{2n}(s)$. If we sample this signal at the times

$$t_k = 10^{-7}[k - (2/\pi)\eta], \qquad (6)$$

we get a sequence of sample values of the form $s(t_k) = \{Q_0, I_1 - Q_2, -I_3, Q_4, \cdots\}$ where

$$Q_k = A\sin\{\beta\, m[t_k - \delta(t_k)]\} \text{ (with k = even integers)} \qquad (7)$$

and

$$I_k = A\cos\{\beta\, m[t_k - \delta(t_k)]\} \text{ (with k = odd integers).} \qquad (8)$$

Since the sine function in Eq. (7) is well approximated by $\beta\, m[t_k - \delta(t_k)]$, the Q_k samples contain the information needed to form an estimate of the delayed PRN ranging signal. It can also be shown that the expected value of the I_k samples is $AJ_0(b)$, so the I_k samples provide an estimate of signal amplitude.

Unfortunately, the sampling times given in Eq. (6) require nanosecond-level control of the rising edge of the strobe signal going to the RRC's A/D-converter, and achieving that level of control would have required more PC board space and electrical power than was available on the New Horizons spacecraft. The solution we adopted was to precede the RRC's DLL tracking phase with a clock alignment phase in which sampling sequences of the form

$$t_k = \frac{n}{30 \times 10^6} + 10^{-7} k, \qquad (9)$$

where n is an integer between 1 and 12, are tried until the sequence giving the largest mean value of I_k is found. In effect, what happens is the system first counts-out n zero-crossings of the USO output signal and then forms the A/D strobe signal by taking every third zero-crossing after that. This procedure gives us a resolution on t_k of 33-1/3 nanoseconds. The value of n that maximizes I_k will be n = floor[12.5 – (6/π)h], and when the t_k values given by Eq. (9) are inserted into Eq. (5), we get Q_k and I_k samples of the form

$$Q_k = A \sin\left\{\psi + \beta \, \mathrm{m}\left[\mathrm{t_k} - \delta(t_k)\right]\right\} \qquad (10)$$

and

$$I_k = A \cos\left\{\psi + \beta \, \mathrm{m}\left[t_k - \delta(t_k)\right]\right\}, \qquad (11)$$

where ψ is the phase residual between η and the compensation provided by the clock alignment procedure. A plot of ψ as a function of η is given in Fig. 7. Note that ψ never exceeds 15° in absolute value. Fortunately, the impact of ψ on DLL tracking quality is fairly minimal.

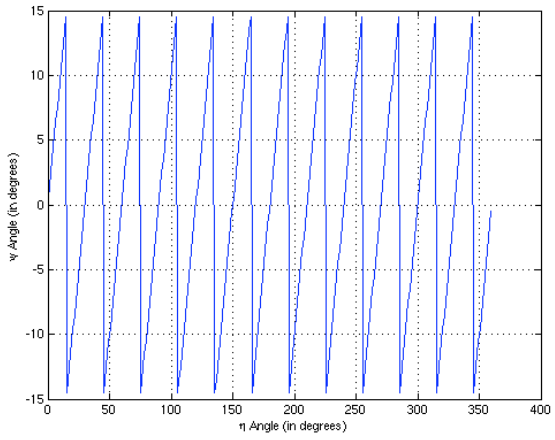

Figure 7. Plot of ψ as a function of η, which is the residual angle error after the clock alignment procedure has finished.

The uplink receiver AGC loop will periodically adjust the IF amplifier gain so that the RMS amplitude of the signal at the output of the narrowband filter, $H_{2n}(s)$, is held constant at 106 millivolts. However, the RMS amplitude of the signal at the output of the wideband filter, $H_{2w}(s)$, will not be constant because at low signal levels when noise predominates, the output of the wideband filter is magnified by the wide/narrow bandwidth ratio; whereas at high signal levels the two filters respond equally. Fig. 8 shows how the amplitude of the signal and noise components of Q_k and I_k behave as the RF input power into the uplink receiver varies over the range of values that are expected for the New Horizons mission.

Delay-Locked Loop. A block diagram of the RRC's delay-locked loop is shown in Fig. 9. The configuration is strongly influenced by the cross-correlation properties shown in Fig. 4. Since C(i) is dominated by the $C_1(i)$ component (an alternating sequence of 1's and 0's) the modulating function is well approximated by the sine-wave $\mathrm{m}(t) \approx \sin \omega_{\mathrm{m}} t$, where $\omega_{\mathrm{m}} = 2\pi f_{\mathrm{m}}$ and f_{m} = (chip rate)/2 = 1,034,733.5435 Hz. The Q_k samples at the input to the DLL will therefore be approximated by

$$Q_k \approx A \sin\left\{\psi + \beta \sin\left[\omega_{\mathrm{m}} \, \mathrm{t_k} + \theta_{\mathrm{m}}(t_k)\right]\right\}, \qquad (12)$$

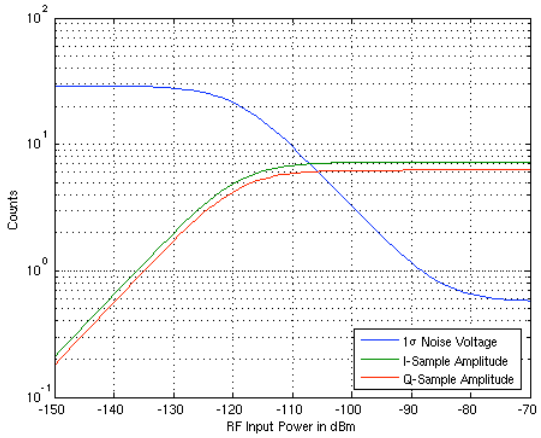

Figure 8. Signal and noise amplitudes in the Q_k and I_k samples.

where $\theta_{\mathrm{m}}(t) = -\omega_{\mathrm{m}} \delta(t)$. Precise (but ambiguous) estimation of the uplink time delay can therefore be obtained by tracking the phase of m(t) with a phase-locked loop. The RRC uses a discrete-time digital 2nd-order type-1 loop. Steady biases in range-rate therefore result in a steady-state phase error of zero. The loop consists of a phase detector, loop filter, number-controlled oscillator, and a C_1(advanced by 90°) component code generator. The sampling frequency will be {100, 25, or 6.25} Hz depending on the tracking mode. For mode {0, 1, or 2}, the loop bandwidth will be {4.0, 1.0, or 0.25} Hz when the RF input power is –138 dBm. Mode 0 will be used for acquisition, mode 1 for normal tracking, and

mode 2 for tracking when the RF input power is less than –135 dBm.

The number-controlled oscillator generates a clock signal that causes the component code generator to generate the signals

$$\hat{C}_1(\text{advanced}) = \mathrm{X}(t_k) = \mathrm{sgn}\left\{\cos\left[\omega_\mathrm{m} t_k + \varphi_\mathrm{m}(t_k)\right]\right\} \tag{13}$$

and

$$\hat{C}_1(k) = \mathrm{sgn}\left\{\sin\left[\omega_\mathrm{m} t_k + \varphi_\mathrm{m}(t_k)\right]\right\}, \tag{14}$$

where $\varphi_\mathrm{m}(t)$ is the loop's estimate of $\theta_\mathrm{m}(t)$.

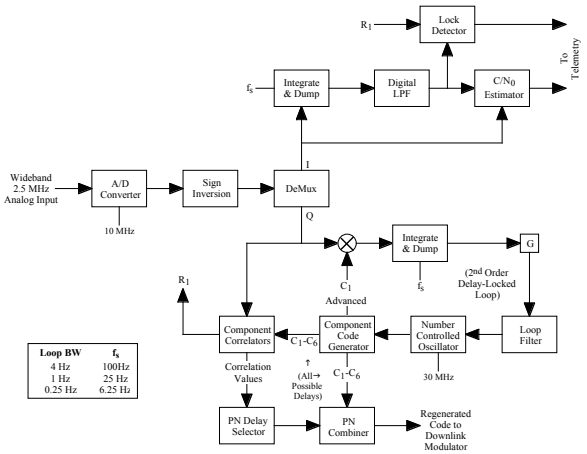

Figure 9. Block diagram of the regenerative ranging circuit delay-locked loop.

Note that component code generators $\hat{C}_2(k)$ - $\hat{C}_6(k)$ are triggered by the same signal that triggers $\hat{C}_1(k)$, so all of the "on-time" code generators change state at the same time. The phase detector generates phase error from the average value of the product of Q_k and $X(t_k)$. It can be shown that this average is equal to

$$\mathrm{e}(t_k) = \mathrm{Ave}\left\{Q_k X(t_k)\right\} = K_\mathrm{d} \sin\left[\theta_\mathrm{m}(t_k) - \varphi_\mathrm{m}(t_k)\right], \tag{15}$$

where $K_\mathrm{d} = (4/\pi) A \mathrm{J}_1(\beta)\cos\psi$ is the phase detector's gain constant. The loop filter is a discrete-time equivalent of the continuous-time transfer function $\mathrm{F}(s) = G(s+a)/s$, where the parameters G and a are chosen so that the loop will have a damping ratio of $\zeta = 1/\sqrt{2}$ and a noise-equivalent bandwidth as specified above. The number-controlled oscillator is a 35-bit phase accumulator with a clocking frequency of 30 MHZ (see Fig. 10).

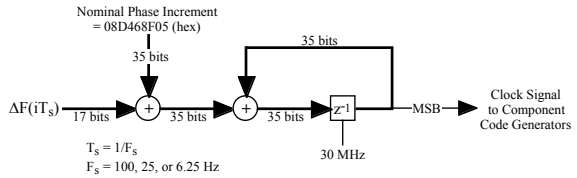

Figure 10. Block diagram of the number controlled oscillator.

This gives the RRC a range-rate resolution of 0.126 m/s and a range resolution of {0.126, 0.506, or 2.024} cm for tracking modes {0, 1, or 2}. The loop is capable of tracking signals with range-rates up to ±4144 m/s and can acquire signals with range-rates up to ±898 m/s without slipping cycles. The code generator is configured to generate and correlate all phases of all six component generators (a total of 77 signals). It then chooses the phase with the largest correlation product (for each component) and forms the composite regenerated code. The Actel chip on which the system is implemented has a total of five correlators that are time-shared in order to form the 77 correlation products. The system also has a lock detector circuit and a circuit for estimating the C/N_0 ratio of the RRC's input signal. The outputs of these circuits go to the RRC's telemetry stream.

RRC Performance. Since the gain of the phase detector is proportional to signal amplitude, the open-loop gain of the DLL is not constant. The z-plane root-locus of the closed-loop poles as the open-loop gain varies from zero to infinity is shown in Fig. 11.

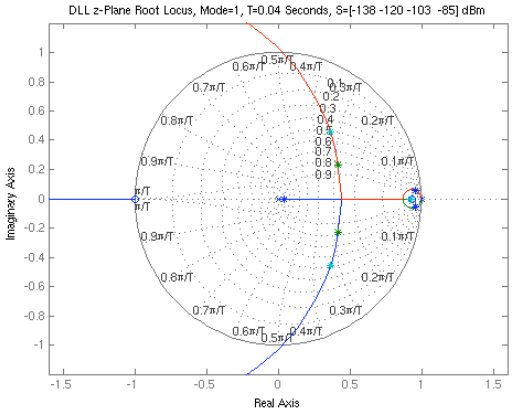

Figure 11. Root-locus plot of the RRC's delay-locked loop when the tracking mode is equal to 1. Marked points

are the closed-loop pole locations when the RF input power is equal to {-138, -120, -103, and –85} dBm.

The locations of the poles at four particular RF input amplitudes are also marked. This movement of the closed-loop poles causes the damping ratio and equivalent noise bandwidth of the loop to vary as a function of the RF input amplitude. These relationships are shown in Figs. 12(a,b). The power spectral density of the noise at the input to the DLL is shown in Fig. 13.

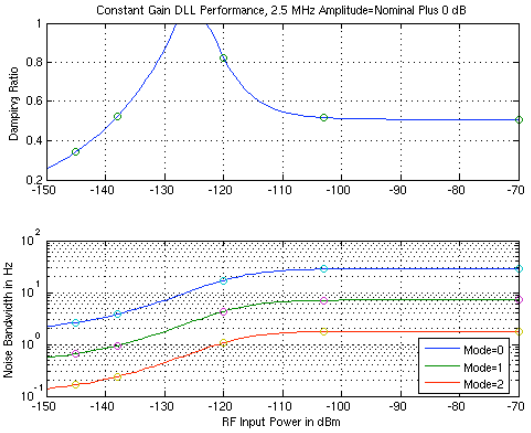

Figure 12. (a) DLL damping ratio as a function of RF input amplitude. (b) Equivalent noise bandwidth of the DLL as a function of RF input amplitude.

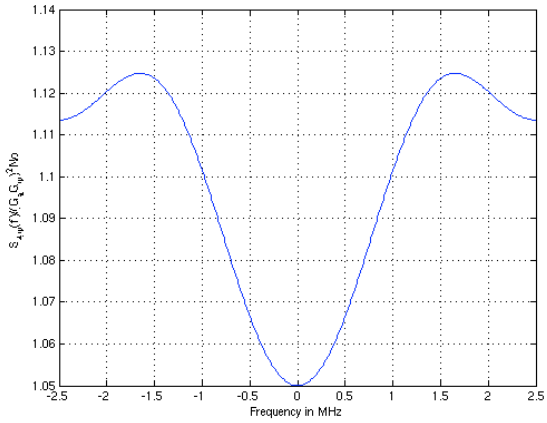

Figure 13. Power spectral density of the noise at the input to the DLL.

The loop acts as a LPF that passes a very small segment of this spectrum near f=0 with width equal to twice the noise equivalent bandwidth of the DLL. The total noise power at the output of the tracking loop will therefore be equal to

$$\sigma_{\varphi}^2 = 2BW \times 1.05\left(G_a G_w\right)^2 N_0 \text{ radians}^2. \qquad (16)$$

A plot of σ_{φ} (converted to meters of range uncertainty) as a function of RF input amplitude is given in Fig. 14. The baseline uplink coverage plan for New Horizons will have received RF power levels in the range of [-138 to -118] dBm, so the corresponding range uncertainty will be [1.77 to 0.44] meters for mode 1 tracking and [0.88 to 0.22] meters for mode 2 tracking.

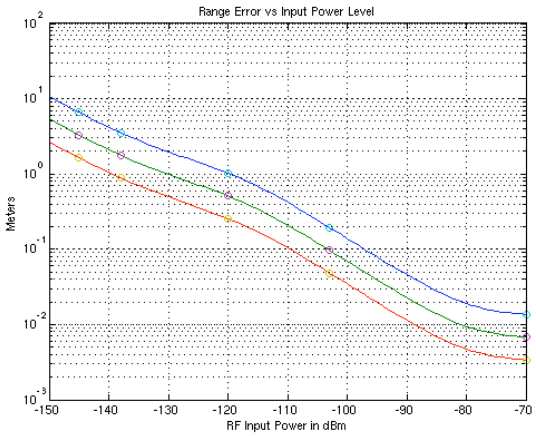

Figure 14. 1σ tracking noise at the output of the RRC's DLL as a function of RF input power. Legend: blue curve – BW=4 Hz, green curve – BW=1 Hz, red curve – BW=0.25 Hz.

Alternate coverage plans result in a somewhat wider range of received RF power levels of [-142 to –103] dBm, and the corresponding range uncertainties will be [2.49 to 0.097] meters for mode 1 tracking and [1.25 to 0.048] meters for mode 2 tracking. These uncertainty levels are well below the New Horizons requirement of 20 meters (1σ) for measurement of two-way range, and allow for most of that requirement to be allocated to the measurement of downlink range.

IMPLEMENTATION

A picture of one of the two Radiometrics flight cards is shown in figure 15. The circuit area used by the RRC is designated in the picture. As was stated previously, the entire signal processing for the RRC, except for the analog digital conversion, was contained within an Actel RT54SX72S FPGA. The analog to digital conversion was

performed by a Maxwell 9240LP which provided a 14 bit sample of the 2.5 MHz.

The digital design of the circuit was programmed using VHDL and contained all of the algorithms outlined in the theory presented previously in this document. In addition, a serial interface to provide commanding of the circuit and telemetry out of the circuit was implemented. The circuit telemetry contained information about the circuit mode, and tracking status. Data on the state of the NCO, code generators, code selection taps, and the SNR calculated by the circuit were generated at a 1 second rate.

One of the major challenges of this design was getting the whole regenerative ranging tracker to fit within a single FPGA. Many digital circuit optimization techniques were used to minimize FPGA resource usage. FPGA resource also determined the number of code correlators in the final circuit. Reducing the number of correlators translated into longer code acquisition times. The final design settled on 5 code correlators with a acquisition time of 5 minutes for high SNR signals and 30 minutes for low SNR signals. The final design utilized 72% of the registers and 80% of the combinatorial resources of the FPGA.

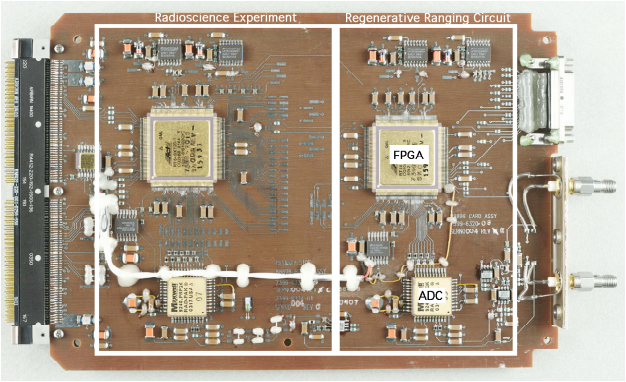

Figure 15. Radiometrics Card

PERFORMANCE

Testing and characterization of the RRC has been performed in both stand-alone bench level testing and integrated with the total RF telecommunications system. The two metrics that characterized the performance of the RRC during testing were the mean and standard deviation of the delay between the replica code and the received code. A diagram illustrating how the delay was determined is show in figure 16. The delay is the time from one chip edge within the received PN sequence with the corresponding chip edge in the replica code.

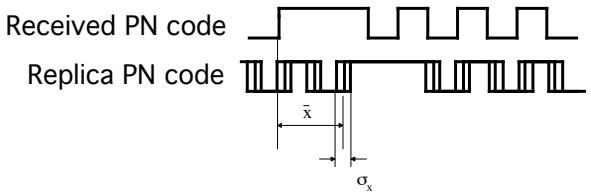

Figure 16. RRC Delay Metric

Test data was generated by measuring the time delay between the original PN code and the replica code generated by the RRC. The mean and standard deviation of this data were calculated and plotted against the RF power. These measurements were repeated for changes in temperature, modulation index and carrier frequency offset from the nominal. The metrics were measured over a RF received power range of –90 dBm to –140 dBm. Figure 17 shows the standard deviation of the delay for both tracking loop bandwidths. Figure 18 shows the calculated mean of the delay over the RF power range. The theoretical performance is shown as dashed lines whose color corresponds to the respective tracking bandwidth.

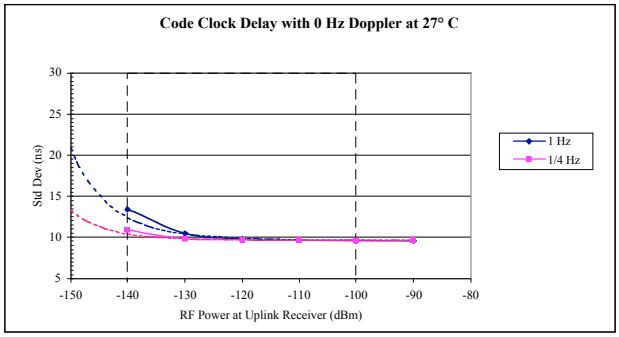

Figure 17. Code Clock Jitter

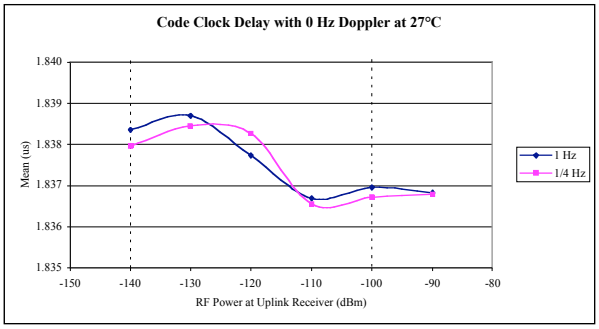

Figure 18. Code Clock Mean

The code deviation requirement for the code clock delay for the New Horizons mission was set at 30 ns. The implemented circuit is well within this range for it's designated operating range. The variation of the mean code clock delay was less than 2 ns over the operating range of the circuit.

The RRC also contains a circuit that approximates a signal to noise ratio for the received code. A plot of the pseudo-SNR measured by the RRC is shown in figure 19. This SNR measurement is optimized to have the most sensitivity within the expected operational range of the RRC. There are three traces that represent the SNR during the various stages of development and testing of the RRC. The lines represents the SNR measured with the prototype board, the flight board during bench testing, and the flight board integrated with the uplink receiver.

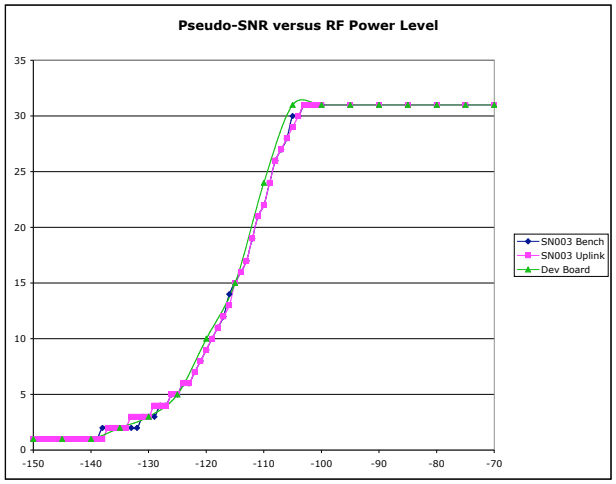

Figure 19. Pseudo-SNR Measured by the RRC

As part of the diagnostic and testing of the RRC, pre-flight RRC FPGAs had the capability to report the individual code accumulation values of the code correlators. Figures 20 and 21 show the code accumulations for the C3 code at a power level of –120 dBm and –138 dBm.

As expected the peak of the higher power signal is more clearly defined than the lower power signal. But even the peak of the lower power signal is clearly defined. The algorithm that selects the code taps for the circuit is designed with some hysterisis built in.

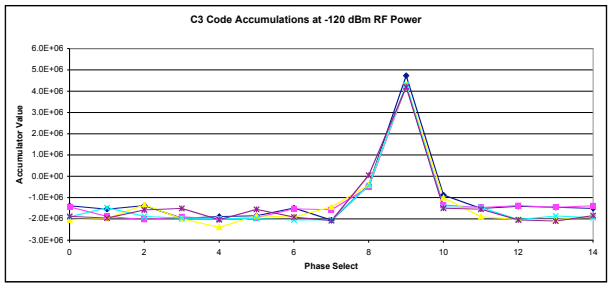

Figure 20. C3 Code accumulation at –120 dBm

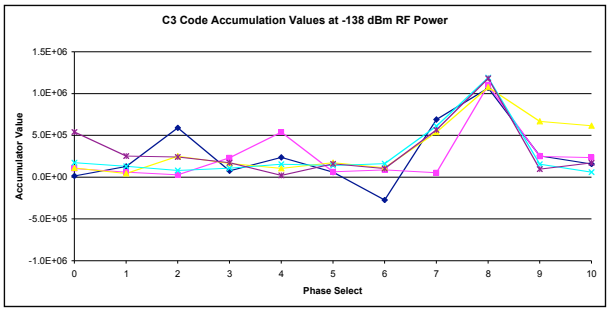

Figure 21. C3 Code Accumulations at –138 dBm

The circuit will not change a code tap unless the last three code taps are all the same. This way once a series of code taps were selected they would stay relatively constant and wouldn't change every correlation cycle. The reasoning was that any change in individual code taps has a dramatic impact on the code sequence. This would disrupt any correlation attempts on the ground. So even though it would make code acquisition more difficult and time consuming, the resultant code tap selections would have a higher probability of being correct and moving off this selection would much more difficult. It would also reduce the amount of times the code sequence would jump around.

SUMMARY

This paper discussed a Regenerative Pseudonoise Ranging Tracker for the New Horizons spacecraft. This type of ranging technique reduces the amount of noise on the tracking signal received back on the ground. An overview of the RF telecommunications system for New Horizons was presented as well as the RRC's place within that system. A brief introduction to traditional tracking of interplanetary spacecraft was presented. A more detailed discussion of regenerative ranging using a pseudonoise code was outlined. The characteristics of the PN code were covered in some detail. A thorough theoretical discussion of the regenerative ranging tracker for New Horizons was also presented as well as the expected performance of the tracker. The implementation of the circuit was briefly discussed and some results of the flight circuit were presented.

ACKNOWLEDGMENTS

We would like to thank the New Horizons Project Office for their support of this endeavor. We would like to especially thank Glen Fountain (project manager) and Chris Hersman (spacecraft systems engineer) for their support in making this circuit a reality. We would also like to thank many of the engineers whose talents were called upon to help in the design and testing of this circuit Laurel Funk, Chris Britt, Paul Grunberger, Bob Jensen, Wes Millard, Ballard Smith, Lloyd Linstrom, Kim Strohbehn and Michael Vincent.

REFERENCES

[1] H. W. Baugh: "Sequential Ranging – How It Works", JPL Publication 93-18, Jet Propulsion Laboratory, California Institute of Technology, Pasadena CA, 15 June 1993.

[2] P. W. Kinman: "(202) 34-m and 70-m Doppler", 810-005, Rev E, DSMS Telecommunications Link Design Handbook, 15 November 2000.

[3] R. W. Sniffin: "(203) Sequential Ranging", 810-005, Rev. E, DSMS Telecommunications Link Design Handbook, 11 December 2000.

[4] J. B. Berner and S. H. Bryant: "Operations Comparison of Deep Space Ranging Types: Sequential Tone vs. Pseudo-Noise", IEEE 2002 Aerospace Conference Proceedings, vol. 3, pp. 3-1313 – 3-1326, 9-16 March 2002.

[5] J. B. Berner, J. M. Layland, P. W. Kinman, and J. R. Smith: "Regenerative Pseudo-Noise Ranging for Deep-Space Application", TMO Progress Report 42-137, 15 May 1999.

[6] P. W. Kinman: "(214) Pseudo-Noise and Regenerative Ranging", 810-005, Rev E, DSMS Telecommunications Link Design Handbook, 30 April 2003.

[7] J. R. Jensen and R. S. Bokulic: "A Highly Accurate, Noncoherent Technique for Spacecraft Doppler Tracking", IEEE Transactions on Aerospace and Electronic Systems, **35**, 3 (July 1999), 963-973.

[8] J. R. Jensen and R. S. Bokulic: "Experimental Verification of Noncoherent Doppler Tracking at the Deep Space Network", IEEE Transactions on Aerospace and Electronic Systems, **36**, 4 (October 2000), 1401-1406.

[9] C. C. DeBoy, C. B. Haskins, T. A. Brown, R. C. Schulze, M. A. Bernacik, J. R. Jenson, W Millard, D. J. Duven and S. Hill. "The RF Telecommunications System for the New Horizons Mission to Pluto" , IEEE 2004 Aerospace Conference Proceedings, vol 3. 6-13 March 2004

[10] C.B. Haskins and W.P. Millard. "X-Band Digital Receiver for the New Horizons Spacecraft", IEEE 2004 Aerospace Conference Proceedings, vol 3. 6-13 March 2004